BIOINFORMATICS AND BIOMEDICAL RESEARCH JOURNAL
2019, Vol. 2, No. 1, 12–20
http://dx.doi.org/10.11594/bbrj.02.01.03

Research Article

The Binding Prediction Model of The Iron-responsive Element Binding Protein and Iron-responsive Elements

The Binding Prediction Model of the IRP and IRE

Kevin Nathanael Ramanto, Arli Aditya Parikesit*

Department of Bioinformatics, School of Life Sciences, Indonesia International Institute for Life Sciences, Jakarta 13210, Indonesia

Article history:
Submission October 2019
Revised December 2019
Accepted December 2019

**Corresponding author:*
E-mail: arli.parikesit@i3l.ac.id

ABSTRACT

Iron is essential to fulfilling an indispensable role in the biological process in human physiology. Various proteins were known involved in iron metabolism. One of the proteins called iron-responsive element-binding protein (IRP) which acts as a master iron of cellular iron homeostasis. There are two IRP known to date, which is: IRP1 and IRP2. Previous studies showed IRP bind to iron-responsive elements (IRE) located in 5'-UTR of the transferrin receptor 1. The interaction of IRP/IRE is well studied through many years to find a better treatment for the cellular disorder in iron metabolism. However, the structural differences of both IRP and the binding prediction model of IRP/IRE remain unclear. This study provides a better understanding of the IRP structure and the IRP/IRE2 binding prediction model in a healthy condition. Several bioinformatic analyses were implemented in this study, such as molecular docking simulation, domain prediction, and structural similarity analysis. Structural analysis of IRP demonstrates a low root mean square deviation score that indicates both of IRP have high similarity in structure with different characteristics, such as binding sites and metabolic pathway. Interestingly, molecular docking simulation showed IRP1 interaction is more stable than IRP2. Thus, this information could be beneficial in developing a drug for an iron-related disease.

Keywords: iron metabolism, iron-responsive element binding protein, iron-responsive element, molecular docking simulation

Introduction

Iron is essential for fulfilling an indispensable role in various biochemical processes in humans, such as DNA replication, repair, and translation [1]. One of the main functions of the iron is to involve the oxygen-binding characteristic of porphyrin complexed iron, which is essential for the oxygen-carrying capacity of myoglobin and hemoglobin [1]. Thus, a cellular disorder in iron metabolism may have severe consequences for human health. Insufficient iron supply will lead to a shortage of healthy red blood cells and resulting in iron deficiency anemia or known as ferropenic. On the contrary, iron overloading could damage various organs and lead to diseases, such as diabetes, cancer, and heart disease [1].

Several proteins are involved in maintaining iron metabolism. One of them is the iron-responsive element-binding proteins (IRPs) that act as master regulators of cellular iron homeostasis [2]. Furthermore, IRPs have known to maintain the rate of mRNA translation by binding to a stem-loop mRNA structure known as iron-responsive elements (IREs) [3].

IREs usually contain 30 nucleotides folded into RNA helices which are separated by a mid-

How to cite:
Ramanto KN, Parikesit AA (2019) The Binding Prediction Model of The Iron-responsive Element Binding Protein and Iron-responsive Elements. Bioinformatics and Biomedical Research Journal 2 (1): 12– 20. doi: 10.11594/bbrj.02.01.03.

helix bulge cytosine residue and six nucleotide loops [4]. The model for IRPs/IREs was first to discover by Haile et al. in 1989 [5]. The analysis also reveals that IRPs exist in two states by implementing a gel retardation assay to IRP/IRE [5]. There are two closely related IRPs that have known to date, which are IRP1 and IRP2. IRP1 has identified as a bifunctional protein that switching between RNA binding and aconitase depending on the conditional iron level. In the Iron low-level condition, IRP1 will inhibit the translation of ferritin by binding to the IREs that located in the 5'-UTR of transferrin 1 (TFR1) mRNA [3]. The binding of IRE with IRP occurs through bonds made to the terminal loop and stem interrupting C through two separate binding sites [6]. In Iron high-level condition, IRP1 is enzymatically active and no longer binds well to IREs, which leads to the degradation of TFR1 mRNA. On the other hand, IRP2 does not have enzymatic activity and responds to iron by induced iron starvation. Similar to IRP1, IRP2 binds to IREs with high affinity in low iron conditions [3].

TFR1 is an expressed transmembrane protein known for its function in transferrin-bound iron uptake in various cell types. TFR1 is composed of two disulfide-bonded subunits. Furthermore, it also contains three N-linked glycan units and posted translationally modified with fatty acyl groups and phosphate [3]. Within 5'-UTR of TFR1, there are known five stem-loop structure of IREs [5]. Previous studies have shown the interaction between IRPs and IRE. The research conducted by Khan et al. provided thermodynamic and kinetics analysis of IRP1 and IRE [6]. Their study discovers changed RNA conformation upon IRP1 binding, and decreased RNA hydrogen bonding are influenced by the thermodynamics and kinetics and kinetic selectivity of the protein or RNA interaction [6].

Even though the interaction of IRP and IRE is well studied in many years, the differences between IRP1 and IRP2 when binding to IREs remain unclear. It is known that IRP1 and IRP2 have a different pathway in iron metabolism and will act differently in high iron conditions [3]. Therefore, the binding model of the IRP1 and IRP2 should be different. One of the reasons for these differences may cause by the protein-specific characteristic in each of IRPs. The differences in IRP-IRE binding models may help to uncover the truth in iron homeostasis and support drugs for iron-related diseases. The main objective of this study is to provide a better insight into the binding model of IRP-IRE complexes in humans by implementing molecular docking simulation. The protein-specific characteristics in IRPs were analyzed by using reliable bioinformatics tools. As a result, this study can provide a better understanding of the IRP binding mechanism to IRE.

Methods

Data Retrieval

Three fasta files were obtained from the GenBank (https://www.ncbi.nlm.nih.gov) which are IRP1 and IRP2 amino acid sequences; and TFR1 nucleotide sequence. All the sequences are related to Homo sapiens. The search of the sequences was done on 17th June 24, 2019, with the keywords "Iron-responsive element-binding protein Homo sapiens" for IRP sequences and "Transferrin receptor mRNA Homo sapiens" for transferrin nucleotide sequence. The specific accession number and the length of each sequence were described in Table 1.

IRPs and IREs Structure Prediction

Both of the IRP 3D protein structures were predicted by using a protein fold recognition webserver called PHYRE2 (http://www.sbg.bio.ic.ac.uk/phyre2/) [7]. Each of the amino acid sequences of IRP was uploaded to PHYRE 2 server, and 2 PDB files of IRPs were obtained. The structure prediction with the PHYRE2 server was run for 6 hours with normal mode. IREs within TFR1 were predicted by using SIREs web server 2.0 (http://ccbg.imppc.org/sires/index.html) [8]. SIREs is a sequence searcher based on the Perl based-program that predicts IREs within the RNA or DNA sequence [8]. After the sequences of IREs

Table 1. Sequences detail information

Accession Number	Protein/Nucleotide Sequence Name	Length
P21399	IRP1	889 aa
P48200	IRP2	963 aa
NM_001128148	TFR1	5,012 bp

were obtained, the RNAfold web server (http://rna.tbi.univie.ac.at/cgi-bin/RNAWeb-Suite/RNAfold.cgi) was used to predict the secondary structure of each IREs [9]. The predicted secondary structures from RNAfold web server were used as parameter to predict 3D model of IRE. The 3D structure of IREs was predicted by using simRNA (https://genesilico.pl/SimRNAweb/submit) where the number of steps simulation was set to 1000 in each IRE prediction to test RNA structures robustness [10].

Protein Analysis

In order to analyze the differences of IRPs properties, several protein analysis was done in this study. Domain analysis and post-translational modification (PTM) site prediction were conducted to determine the protein function and activity. IRPs domain were predicted with InterPro (https://www.ebi.ac.uk/interpro/) where predicted domain and its location were recorded [11]. Meanwhile, PTM prediction was done by using ModPred (http://www.modpred.org) where only PTM sites categorized has high confidence level were recorded [12]. The iPBA web server (http://www.dsimb.inserm.fr/dsimb_tools/ipba/) was used to do structural similarity analysis where the global alignment was set as the parameter for the alignment type [13]. The similarity and aligned score were recorded. The RNA binding site prediction was done by using a DRNApred web server (http://biomine.cs.vcu.edu/servers/DRNApred/) to determine the probabilities of RNA-protein interaction [14]. Lastly, the protein-protein network of IRP-1 and IRP-2 from *Homo Sapiens* were searched in the STRING database (https://string-db.org) to determine the pathway of activation for both of IRPs [15].

Molecular Docking Simulation

The interaction of IRP-IRE were further investigated by conducting molecular docking simulation procedure. Molecular docking simulation between IRPs and IREs was done by using PatchDock Server (https://bioinfo3d.cs.tau.ac.il/PatchDock/) where the Root Mean Square Deviation (RMSD) was set to 4Å [16]. The docking method of Protein-RNA or protein-protein complex was said to be proper if the RMSD value was smaller or equal to 5Å. If the RMSD value obtained was greater than 5Å, it means that the method used cannot be trusted [17]. Therefore the PatchDock server was recommended to set RMSD equal to 4Å for protein-RNA docking [16]. The molecular interaction between IRPs and IREs was visualized by using PDBsum Generate (http://www.ebi.ac.uk/thornton-srv/databases/pdbsum/Generate.html) [18]. Each binding prediction model with lowest free energy that indicated high interaction were recorded and presented in this study. The benchmark of IRP and IRE binding was checked in three published benchmarks to validate predicted IRP-IRE binding models. They were the protein-RNA docking benchmark v1.1 from the Fernandez-Recio group [19], the protein-RNA docking benchmark version 2 from the Bahadur group [20], and the protein-RNA docking benchmark 1.0 by the Zou group [21], respectively.

Results and Discussion

IRPs and IREs Structure Prediction

As seen in figure 1, there is no significant difference between IRP1 and IRP2 were found. This indicates that both of the IRPs have a high similarity rate with each other. According to Berric R. Henderson [22], IRP1 and IRP2 share 79% similarity on amino acid sequences even though both IRPs encoded by genes on the different chromosomes. Despite IRPs' high similarity in the structure, IRPs will act differently in a high iron condition where IRPs will not bind to IREs.

Five different IREs were found in TFR1 and named according to their location order. This finding was similar to Casey et al. that found 5 IREs in TFR1 back in 1988 [23]. Each of the IREs consists of 31 nucleotides where all of them were found in 3238-3835 nucleotide position of TFR1 (table 2). The minimum free energy (mfe) score of all of IREs was negative where IRE5 has the lowest mfe score (table 2). This may indicate that IRE5 is the most stable structure compare to other IREs.

Figure 2 shown that IRE1, IRE2, and IRE3 have a similar structure, while IRE4 and IRE5 have a unique lower helix structure. The terminal loop of each IREs consists of “CAGNGN” nucleotide sequences where “N” represents any nucleotides. Furthermore, there are five base-pair of nucleotides in the upper helix of IREs. In the mid-stem, there is cytosine bulge that mark by the green circle (figure 2.A).

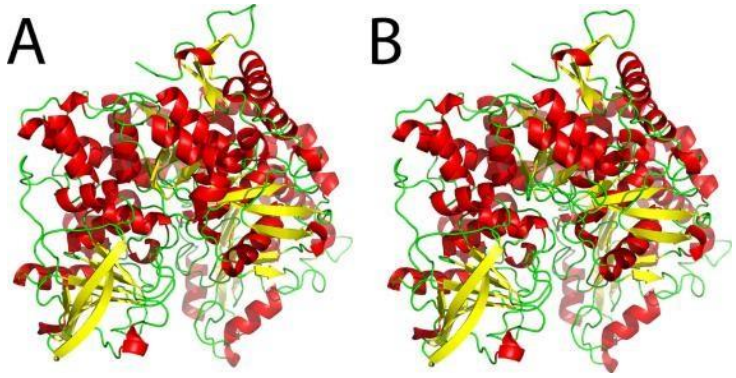

Figure 1. The tertiary structure of IRP1

Table 2. IREs detail information

IRE name	Location	RNA Sequence	mfe
IRE1	3238 - 3269	UAUUUAUCAGUGACAGAGUUCACUAUAAAUG	-6.90
IRE2	3288 - 3319	UAAUUAUCGGAAGCAGUGCCUUCCAUAAUUA	-8.40
IRE3	3692 - 3723	ACAUUAUCGGGAGCAGUGUCUUCCAUAAUGU	-9.80
IRE4	3757 - 3788	UCUGUAUCGGAGACAGUGAUCUCCAUAUGUU	-9.00
IRE5	3804 - 3835	UAAUUAUCGGGAACAGUGUUUCCCAUAAUUU	-11.70

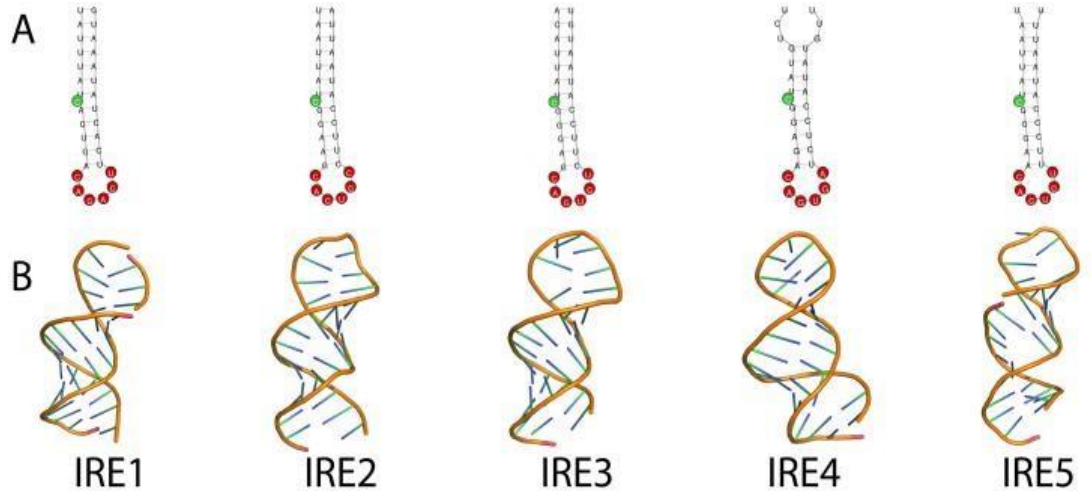

Figure 2. IREs predicted structure in 2D (A) and 3D (B) model

Figure 3. Domain prediction of IRP1 and IRP2 by using Interpro

Protein Analysis

Domain prediction was detected aconitase and swivel domain in both of IRPs (figure 3). Aconitase domain represents the 4Fe-4S cluster binding region, which found at the N-terminal of eukaryotic IRPs [18]. Furthermore, aconitase domain involved in both the glyoxylate and tricarboxylic acid cycles which compromise the first step of oxygen-dependent ATP biosynthesis [24]. On the other hand, the swivel domain was detected at the C-terminal of eukaryotic IRPs (figure 3). This domain has three layers beta/beta/alpha structure and known to rotate between cytosolic form and IRP form [25].

Another similarity of IRPs can be observed in the tertiary structure. To analyse the structural similarity between the IRPs, both of the IRPs were aligned by using iPBA server [13]. The result from iPBA server showed a low RMSD (0.49) with 99.77% residue aligned which indicates the IRPs have related protein folds [13]. Furthermore, the GDT score is extremely high which indicates the IRP1 is homologous to IRP2. The aligned IRP are shown in figure 4 where there are only slight differences that can be observed in the structure.

In PTM prediction, ModPred has detected three residues that undergo amidation in both IRPs which indicate the aconitase activity regulated by means of redox independent PTMs [24]. Not only that, proteolytic cleavage and glycosylation were detected in IRP1 and IRP2 that may play an important role in enzyme activity and stability of IRPs (table 4) [26]. Another impressive result can be seen in IRP2 where O-linked glycosylation and

Table 3. The alignment score of IRP1 and IRP2

Parameter	Score
Normalized score	545.60
RMSD	0.49
Alignment length	882
Aligned residues	880
Fraction aligned	99.77%
*GDT TS	98.93

GDT TS: Global Distance Test

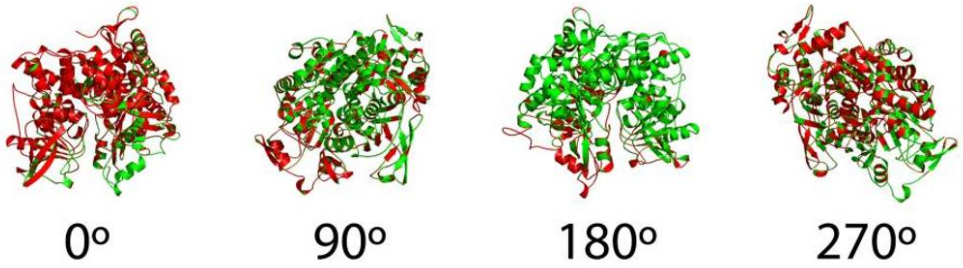

Figure 4. Alignment of IRP1 and IRP2 by using iPBA where red represent IRP1 and green represent IRP2

Table 4. PTM sites prediction of IRP1 and IRP2 by using ModPred

IRP1			IRP2		
Residue	**PTM types**	**Score**	**Residue**	**PTM types**	**Score**
Y319	Proteolytic cleavage	0.434	E396	Amidation	0.065
N442	N-linked glycosylation	0.434	N515	N-linked glycosylation	0.065
G763	Amidation	0.067	N514	N-linked glycosylation	0.065
D345	Proteolytic cleavage	0.063	K568	Methylation	0.064
R344	Proteolytic cleavage	0.063	S545	O-linked glycosylation	0.063
R601	Amidation	0.061	D274	Proteolytic cleavage	0.061
K785	Ubiquitination	0.059	K847	Methylation	0.061
K572	Ubiquitination	0.057	A83	Amidation	0.061
K331	Acetylation	0.057	I299	Amidation	0.061
Y882	Amidation	0.041	R796	Proteolytic cleavage	0.061

methylation were only detected in IRP2 (table 4). O-linked glycosylation is can be described by the interaction of sugar with a hydroxyl group of a serine or threonine. The O-linked glycosylation might influence the slightly structural differences in IRP2. Meanwhile, methylation modifies the nitrogen atom in K568 residue which plays an important role in the gene expression regulation in IRP2 [26]. The differences in detected PTMs in both IRPs may be influencing the differences in aconitase activity. Not only in PTM, but the differences of IRPs can also be observed in the protein-protein network.

According to the StringDB database, both of IRPs have a unique protein-protein network (figure 5) [15]. This indicates that IRP1 and IRP2 have a different pathway of activation. As seen in figure 5, both of IRPs interact with FBXL5 and GLRX3 protein. FBLX5 plays an important role in iron homeostasis by promoting the ubiquination and subsequent degradation of IRP2. In high iron conditions, FBLX5 will bind to IRP2 to promote its ubiquitination and degradation by the proteasome. Meanwhile, GLRX3 is responsible for hemoglobin maturation which activates by IRPs protein [15]. The differences in the PTM characteristics and protein-protein network might influence the interaction between IRP and IRE.

RNA binding prediction score of both IRPs was done to predict which residue likely to interact with IREs. The detail of the RNA binding probability score shown in table 5 where only 10 residues with the highest probability score were recorded [13]. As seen in table 5, residues in IRP1 has a higher binding prediction score compare to IRP2. This may suggest that IRP1 has a higher binding affinity with IREs. Unfortunately, DRNApred did not detect the exact RNA-binding residue in both of IRPs.

Molecular docking Simulation

The result of molecular docking of IRPs and IREs showed in table 6 where all of the binding prediction models have a negative ACE score which indicates there is an interaction that occurs in all models [16].

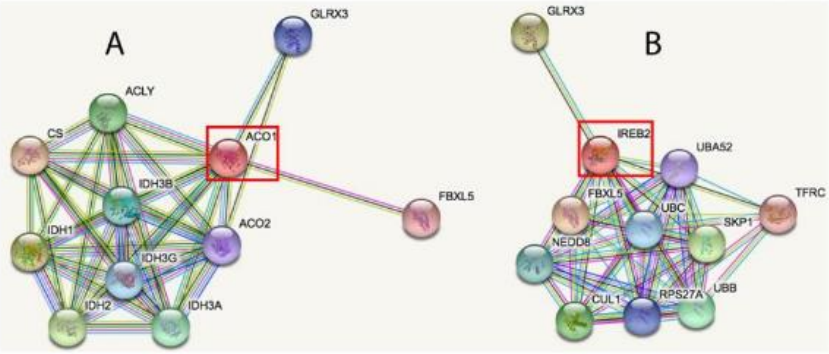

Figure 5. Protein-protein interaction pathway of IRP1 or ACO1(A) and IRP2 or IREB2(B) obtained from the STRING database

Table 5. Ten highest RNA binding site prediction score

IRP1			IRP2		
Residue	**Location**	**Score**	**Residue**	**Location**	**Score**
Met	248	0.13	Arg	43	0.09
Lys	886	0.13	Gly	570	0.09
His	804	0.12	His	879	0.09
Arg	885	0.12	Ile	886	0.09
Lys	79	0.11	Ser	383	0.08
His	126	0.11	Cys	578	0.08
Arg	168	0.11	Ser	628	0.08
His	178	0.11	His	741	0.08
Gly	244	0.11	Lys	877	0.08
Lys	250	0.11	Asp	881	0.08

The geometric shape complementary score of IRE1, IRE2, and IRE3 was higher when binding with IRP1 (table 6). Meanwhile, IRE4 and IRE5 scores were higher when binding with IRP2. These findings may suggest that IRP1 would preferably bind to IRE1, IRE2, and IRE3 while IRP2 preferably bind with IRE4 and IRE5. These findings were supported by the fact that IRP2 is lacks of aconitase activity compare to IRP1 [27]. The overview of each of the binding prediction models shown in figure 6. Even though the position of IREs looked similar, the Protein-RNA interaction of each model is different.

The Protein-RNA interaction of each model is available in Mendeley data (https://data.mendeley.com/datasets/yfxthhhdtp/1) [28]. In IRP1, 21 residues forming a hydrogen bond with IREs, while there are 15 residues in IRP2 that forming a hydrogen bond. Furthermore, the number of the hydrogen bond interactions in RPI is bigger than IRP2 were some of the residues interact with more than one nucleic acid [28]. These findings suggest that the interaction of Protein-RNA in IRP1 is more stable than IRP2. A hydrogen bond is a relatively strong form of intermolecular attraction and plays an important role in the interactions of proteins and nucleic acid [29]. Even though the binding prediction model provides a good result, there are no published benchmarks were found for IRP-IRE docking in humans [19-21]. The protein-RNA docking published benchmarks only provide the benchmark for IRP-IRE in the European rabbit (*Oryctolagus cuniculus*) where the RMSD was bigger than 5Å [19 -21]. This means that there is no suitable benchmark for IRP-IRE docking in human and further research is needed to confirm this study.

Since IRPs are responsible for iron homeostasis, then these binding models may important for finding a suitable drug for iron-related disease. The disruptions of IRP-IRE regulatory system could lead to hyperferritinemia where a patient have an high ferritin levels. Patients that affected by this condition often suffer from neurogenerative disease, such as Alzheimer and Parkinson [30]. Previous studies showed the point mutations

Table 6. Score of IRPs and IREs binding prediction at 4Å

IRP	IRE	Score	Area	ACE* (kcal/mol)	Transformation
1	1	14006	2418.60	- 518.72	-1.28 -0.20 1.10 8.95 -20.51 19.88
1	2	12856	2025.30	- 470.34	-2.11 0.93 -0.42 8.21 -18.48 18.18
1	3	13942	2028.90	- 395.59	-1.85 1.06 -1.75 7.91 -22.27 18.70
1	4	13146	2027.10	- 374.59	-1.07 -0.64 -0.02 7.42 -20.77 21.12
1	5	12574	1973.50	- 397.35	-2.04 1.02 1.27 6.00 -25.76 24.91
2	1	12524	2111.40	- 613.59	-1.29 -0.13 1.00 7.60 -20.86 21.70
2	2	12458	1832.20	- 386.33	-1.84 0.92 -0.50 5.89 -20.90 21.52
2	3	13410	2092.10	- 470.98	-2.02 0.97 -1.67 6.26 -23.81 22.39
2	4	13588	2104.30	- 479.79	-1.07 -0.84 -0.08 7.28 -20.94 21.13
2	5	13480	1685.90	- 329.28	-2.51 1.05 1.84 5.17 -26.98 25.80

ACE: Atomic Contact Energy

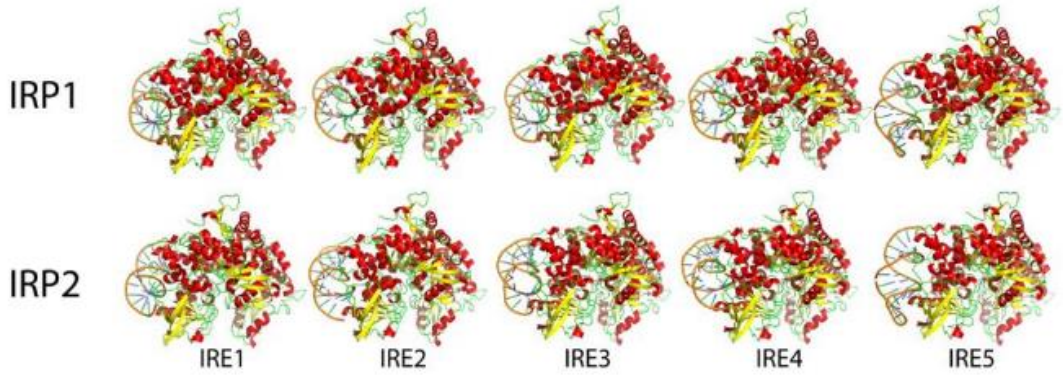

Figure 6. Molecular docking simulation of IRPs and IREs at 4Å by using PathcDock server

of IRPs and IREs in neurodegenerative disease disturb the IRP binding interaction [31]. In order to alleviate the excess iron accumulation, IRE inhibitors drug is currently develop to treat Alzheimer and Parkinson disease [31]. One of the drug known as anthracyclines has been used as IRE inhibitor by binding within the UG wobble pairs flanking and asymmetrically bulged C-residue [32]. However, the development of IRE inhibitor is a challenging task. The basic understanding of IRP-IRE interaction should be uncover to develop a IRE inhibitor drug. The study showed the different binding mechanism and protein properties of IRP1 and IRP2 which important in drug development for neurogenerative disease. Thus, the predicted binding model may provide the benchmark of IRPs and IREs binding mechanisms in healthy condition as well as support the IRE inhibitor drug development in the future.

Conclusion

In summary, the protein analysis of IRP1 and IRP2 suggest that both IRPs have the same functionality, but have a different characteristic in PTM and pathway. Moreover, the predicted binding model showed different behaviour of IRPs when targeting specific IRE where the binding prediction model with IRP1 is more stable than IRP2. These findings may increase our understanding of IRPs and IRE interactions. In the future, these binding models may become useful in the drug discovery field.

Acknowledgment

The author would like to thanks to the Indonesia International Institute for Life Sciences (I3L) for their heartfelt support and providing the funding. Thanks also go to Direktorat Riset dan Pengabdian Masyarakat, Direktorat Jenderal Penguatan Riset dan Pengembangan Kementerian Riset, Teknologi dan Pendidikan Tinggi Republik Indonesia for providing Hibah Penelitian Dasar DIKTI/LLDIKTI III 2019 No. 1/AKM/PNT/2019.

References

1. Crielaard, B. J., Lammers, T. & Rivella, S. (2017). Targeting iron metabolism in drug discovery and delivery. *Nature Reviews Drug Discovery,16* (6):400-423.
2. Thomson, A. M., Rogers, J. T. & Leedman, P. J. (1999). Iron-regulatory proteins, iron-responsive elements, and ferritin mRNA translation. *The International Journal of Biochemistry & Cell Biology,31* (10):1139-1152.
3. Leamon, C. P. & Low, P. S. (2005). Receptor-Mediated Drug Delivery. *Drug Delivery*,167-187.
4. Khan, M. A., Ma, J., Walden, W. E., Merrick, W. C., Theil, E. C & Goss, D. J. (2014). Rapid kinetics of iron-responsive element (IRE) RNA/iron regulatory protein 1 and IRE-RNA/eIF4F complexes respond differently to metal ions. *Nucleic Acids Research,42* (10), 6567-6577.
5. Haile, D. J., Hentze, M. W., Rouault, T. A., Harford, J. B. & Klausner, R. D. (1989). Regulation of the interaction of the iron-responsive element binding protein with iron-responsive RNA elements. *Molecular and Cellular Biology,9* (11), 5055-5061.
6. Khan, M. A., Walden, W. E., Theil, E. C. & Goss, D. J. (2017). Thermodynamic and Kinetic Analyses of Iron Response Element (IRE)-mRNA Binding to Iron Regulatory Protein, IRP1. *Scientific Reports,7* (1).
7. Kelley, L. A., Mezulis, S., Yates, C. M., Wass, M. N. & Sternberg, M. J. E. (2015). The Phyre2 web portal for protein modeling, prediction, and analysis. *Nature Protocols*, *10*:845.
8. Campillos, M., Cases, I., Hentze, M. W. & Sanchez, M. (2010). SIREs: Searching for iron-responsive elements. *Nucleic Acids Research,38* (Web Server).
9. Lorenz, R., Bernhart, S. H., Siederdissen, C. H., Tafer, H., Flamm, C., Stadler, P. F. & Hofacker, I. L. (2011). ViennaRNA Package 2.0. *Algorithms for Molecular Biology,6* (1).
10. Boniecki, M. J., Lach, G., Dawson, W. K., Tomala, K., Lukasz, P., Soltysinski, T., … Bujnicki, J. M. (2015). SimRNA: a coarse-grained method for RNA folding simulations and 3D structure prediction. *Nucleic Acids Research*, *44* (7).
11. Apweiler, R. (2001). The InterPro database, an integrated documentation resource for protein families, domains, and functional sites. *Nucleic Acids Research,29* (1):37-40.
12. Pejaver, V., Hsu, W-L., Xin, F., Dunker, A. K., Uversky, V. N., & Radivojac, P. The structural and functional signatures of proteins that undergo multiple events of post-translational modification Protein Science. 23(8):1077-1093.
13. Gelly, J., Joseph, A. P., Srinivasan, N. & Brevern, A. G. (2011). IPBA: A tool for protein structure comparison using sequence alignment strategies. *Nucleic Acids Research*, *39* (Suppl_2).
14. Yan, J. & Kurgan, L. (2017). DRNApred, fast sequence-based method that accurately predicts and discriminates DNA- and RNA-binding residues. *Nucleic Acids Research*.
15. Szklarczyk, D., Morris, J. H., Cook, H., Kuhn, M., Wyder, S., Simonovic, M., . . . Von Mering, C. (2016). The STRING database in 2017: Quality-controlled protein-protein association networks, made broadly accessible. *Nucleic Acids Research,45* (D1).
16. Schneidman-Duhovny, D., Inbar, Y., Nussinov, R. & Wolfson, H. J. (2005). PatchDock and SymmDock: servers for rigid and symmetric docking. *Nucleic Acids Research*, *33* (Web Server).
17. Huang, S.-Y. (2014). Search strategies and evaluation in protein–protein docking: principles, advances and challenges. *Drug Discovery Today*, *19* (8), 1081–1096.
18. Laskowski, R. A., Jabłońska, J., Pravda, L., Vařeková, R. S. & Thornton, J. M. (2017). PDBsum: Structural summaries of PDB entries. *Protein Science*, *27* (1), 129–134.
19. Pérez-Cano, L., Jiménez-García, B. & Fernández-Recio, J. (2012). A protein-RNA docking benchmark (II): Extended set from experimental and homology modeling data. *Proteins: Structure, Function, and Bioinformatics*.
20. Nithin, C., Mukherjee, S. & Bahadur, R. P. (2016). A non-redundant protein-RNA docking benchmark version 2.0. *Proteins: Structure, Function, and Bioinformatics*, *85* (2), 256–267.
21. Huang, S. Y.& Zou, X. (2012). A nonredundant structure dataset for benchmarking protein-RNA computational docking. *Journal of Computational Chemistry*, *3* (4), 311–318.

22. Henderson, B. R. (1966). Iron Regulatory Proteins 1 and 2. *Bio Essays*, *18* (8), 739–749.
23. Casey, J. L., M. W. Hentze, D. M. Koelier, S. W. Caughman, T. A. Rouault, R. D. Klausner, & J. B. Harford. 1988. Iron-responsive elements: regulatory RNA sequences that control mRNA levels and translation. Science 240:924-928.
24. Lushchak, O. V., Piroddi, M., Galli, F. & Lushchak, V. I. (2013). Aconitase post-translational modification as a key in linkage between Krebs cycle, iron homeostasis, redox signaling, and metabolism of reactive oxygen species. *Redox Report*, *19* (1), 8–15.
25. Gruer, M. J., Artymiuk, P. J. & Guest, J. R. (1997). The aconitase family: Three structural variations on a common theme. *Trends in Biochemical Sciences*,*22* (1):3-6.
26. Audagnotto, M. & Peraro, M. D. (2017). Protein post-translational modifications: In silico prediction tools and molecular modeling. *Computational and Structural Biotechnology Journal*, *15*, 307–319.
27. Piccinelli, P. & Samuelsson, T. (2007). Evolution of the iron-responsive element. *Rna*, *13* (7), 952–966.
28. Ramanto, Kevin Nathanael; Parikesit, Arli Aditya (2020), "The Binding Prediction Model of The Iron-responsive Element Binding Protein and Iron-responsive Elements", Mendeley Data, v1.
29. Kim, H., Jeong, E., Lee, S.-W. & Han, K. (2003). Computational analysis of hydrogen bonds in protein-RNA complexes for interaction patterns. *FEBS Letters*, *552* (2-3), 231–239.
30. Recalcati, S., Minotti, G. & Cairo, G. (2010). Iron Regulatory Proteins: From Molecular Mechanisms to Drug Development. *Antioxidants & Redox Signaling*, *13* (10), 1593–1616. doi: 10.1089/ars.2009.2983.
31. Zhou, Z. D. & Tan, E. (2017). Iron regulatory protein (IRP)-iron responsive element (IRE) signaling pathway in human neurodegenerative diseases. *Molecular Neurodegeneration*,*12* (1).
32. Canzoneri, J. C. & Oyelere, A. K. (2008). Interaction of anthracyclines with iron responsive element mRNAs. *Nucleic Acids Research*, *36*(21), 6825–6834. doi: 10.1093/nar/gkn774